20. Duddu SP, Sokoloski TD. 1995. Dielectric analysis in the characterization of amorphous pharmaceutical solids. 1. Molecular mobility in poly(vinylpyrrolidone)-water systems in the glassy state. J Pharm Sci 84:773–776.
21. Barker SA, He R, Craig DQM. 2001. Low frequency dielectric investigations into the relaxation behavior of frozen polyvinylpyrrolidone-water systems. J Pharm Sci 90:157–164.
22. Yoshioka S, Aso Y, Otsuka T, Kojima S. 1995. Water mobility in poly(ethylene glycol)-, poly(vinylpyrrolidone)-, and gelatin-water systems, as indicated by dielectric relaxation time, spin-lattice relaxation time, and water activity. J Pharm Sci 84:1072–1077.
23. Jonscher AK. 1991. Low-frequency dispersion in volume and interfacial situations. J Mater Sci 26:1618–1626.
24. Bone S, Eden J, Gascoyne PRC, Pethig R. 1981. Conduction and dielectric polarization in proteins and molecular complexes. J Chem Soc Faraday Trans 1 77:1729–1732.
25. Careri G, Geraci M, Giansanti A, Rupley JA. 1985. Protonic conductivity of hydrated lysozyme powders at megahertz frequencies. Proc Natl Acad Sci USA 82:5342–5346.
26. Crowley KJ, Zografi G. 2001. The use of thermal methods for predicting glass-former fragility. Thermochim Acta 380:79–93.
27. Boehmer R, Ngai KL, Angell CA, Plazek DJ. 1993. Nonexponential relaxations in strong and fragile glass formers. J Chem Phys 99:4201–4209.
28. Farrar TC, Becker ED. 1971. Pulse and Fourier transform NMR: Introduction to theory and methods. New York: Academic Press.
29. Wada H. 1987. Koubunshi no denkibussei. Tokyo: Shokabo Publishing.
30. Schaefer J, Stejskal EO, Steger TR, Sefcik MD, McKay RA. 1980. Carbon-13 $T_{1\rho}$ experiments on solid glassy polymers. Macromolecules 13:1121–1126.
31. Fujiwara T, Nagayama K. 1985. The wobbling-in-a-cone analysis of internal motion in macromolecules. J Chem Phys 83:3110–3117.

Available online at www.sciencedirect.com
SCIENCE DIRECT
ELSEVIER
International Journal of Pharmaceutics 308 (2006) 183–189
INTERNATIONAL JOURNAL OF PHARMACEUTICS
www.elsevier.com/locate/ijpharm

Pharmaceutical Nanotechnology

Preparation of camptothecin-loaded polymeric micelles and evaluation of their incorporation and circulation stability

Masato Watanabe [a], Kumi Kawano [a], Masayuki Yokoyama [b], Praneet Opanasopit [c], Teruo Okano [c], Yoshie Maitani [a,*]

[a] *Institute of Medicinal Chemistry, Hoshi University, Ebara 2-4-41, Shinagawa-ku, Tokyo 142-8501, Japan*
[b] *Kanagawa Academy of Science and Technology, KSP Bldg. East 404, Sakado 3-2-1, Takatu-ku, Kawasaki-shi, Kanagawa-ken, 213-0012, Japan*
[c] *Institute of Advanced Biomedical Engineering and Science, Tokyo Women's Medical University, Kawada-cho 8-1, Shinjuku-ku, Tokyo 162-8666, Japan*

Received 7 July 2005; received in revised form 7 October 2005; accepted 24 October 2005
Available online 29 November 2005

Abstract

To improve its aqueous solubility and stability in biological fluid, CPT was physically loaded in polymeric micelles. Polymeric micelles were composed of various poly(ethylene glycol)–poly(aspartate ester) block copolymers (PEG-P(Asp(R))). The incorporation and circulation stability of CPT micelles were evaluated by measuring the CPT in micelle using gel-permeation chromatography and by CPT concentration measurement after intravenous injection using HPLC, respectively, in terms of chemical structure of block copolymers. The stability of CPT-loaded micelles in vivo depended on the amount of benzyl esters, and length of PEG in the polymers to a greater degree than it did in vitro. A stable formulation of CPT-loaded micelles was obtained using PEG-P(Asp) with PEG of 5000 (MW), 27 Asp units, and 57–75% benzyl esterification of Asp residue. This CPT-loaded micelles showed about a 17-fold lower blood clearance value than unstable micelles. The CPT-loaded micelles are potentially delivered to tumor sites owing to an extended circulation in the blood stream.
© 2005 Elsevier B.V. All rights reserved.

Keywords: Camptothecin; Polymeric micelles; Long circulating; In vivo stability

1. Introduction

Camptothecin (CPT) is a naturally occurring cytotoxic alkaloid isolated from the Chinese plant *Camptotheca accuminata* (Wall et al., 1966). CPT and some of its analogs have shown a broad spectrum of antitumor activity against many solid tumors in xenografts (Giovanella et al., 1989, 1991). CPT inhibits the enzyme DNA topoisomerase I, initially by noncovalent binding and subsequently by stabilization of the complex through a nucleophilic attack by the enzyme at the acyl position of the CPT lactone ring (Hertzberg et al., 1989). In early clinical trials, CPT was formulated as a water-soluble CPT-Na^+ (Moertel et al., 1972). However, it was later reported that the lactone E-ring is important for cytotoxicity and that the open-ring carboxylated CPT-Na^+ is inactive. The lactone of CPT is converted to carboxylate in a pH-dependent equilibrium (Fig. 1) (Fassberg and Stella, 1992). To overcome the solubility and stability problems of CPT, several approaches have been investigated. Water-soluble CPT analogs have been prepared but the majority of them were less potent in assays both in vitro and in vivo than the parent drug (Wall and Wani, 1995). Therefore, the development of adequate drug carriers is gaining increasing attention. These include methods such as conjugation to polymers (Zamai et al., 2003; Singer et al., 2001), intercalation into liposomes (Burke et al., 1992; Cortesi et al., 1997), solubilization in microemulsions (Cortesi et al., 1997), formation of inclusion complexes with cyclodextrins (Kang et al., 2002) and entrapment in microspheres (Shenderova et al., 1999; Tong et al., 2003). However, concerning long circulation carriers of CPT in blood stream, there was not enough information.

Drug carriers with longer retention time in the blood stream can be delivered to solid tumors site by a passive

* Corresponding author. Tel.: +81 3 5498 5048; fax: +81 3 5498 5048.
E-mail address: yoshie@hoshi.ac.jp (Y. Maitani).

0378-5173/$ – see front matter © 2005 Elsevier B.V. All rights reserved.
doi:10.1016/j.ijpharm.2005.10.030

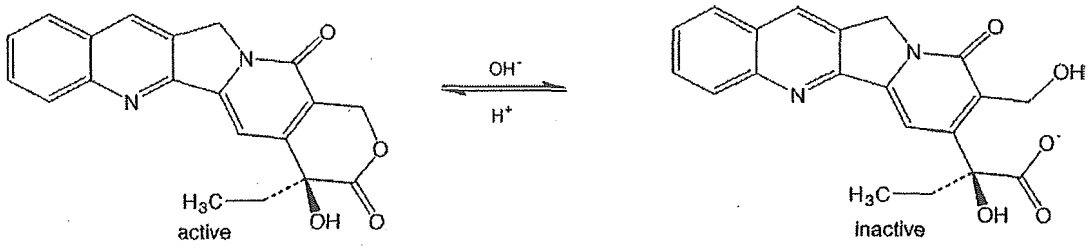

Fig. 1. The structure of camptothecin and equilibrium reaction between the active form and inactive form.

targeting mechanism based on the enhanced permeability and retention effect (EPR effect) (Matsumura and Maeda, 1986; Maeda, 2000; Maeda et al., 2000). Recently, antitumor drug targeting using polymeric micelle carrier systems was achieved with doxorubicin (adriamycin, ADR) using poly(ethylene glycol)–poly(aspartate derivative) block copolymer PEG-P(Asp(R)) (Yokoyama et al., 1987, 1990, 1991, 1998). As a result of selective delivery to tumor site by the EPR effect, dramatically enhanced antitumor effects were obtained in vivo (Yokoyama et al., 1999). In this system, ADR was chemically conjugated to the aspartic acid residue of the block copolymer as hydrophobic species for micelle formation and enhance the physical incorporation of ADR in the inner core. However, the chemically conjugated ADR did not play a role in the expression of anticancer activity (Yokoyama et al., 1999, 1998). Only the physically incorporated ADR expressed selective anticancer activity by being recruited to solid tumor sites.

In previous studies, we reported polymeric micelle system for incorporation of CPT, in which CPT incorporation efficiency and CPT-loaded micelles stability were improved by modification of a hydrophobic segment of the PEG-P(Asp) (Yokoyama et al., 2004; Opanasopit et al., 2004). Chemical structure of block copolymers would largely influence to the stability of polymeric micelles in blood stream. In this study, the in vivo circulation stability of CPT-loaded micelles was evaluated in terms of copolymer composition (PEG length, Asp unit number, ester groups, and esterification degree) and feeding ratio of the drug to copolymer, and compared with incorporation stability of CPT. CPT-loaded micelles with a stable copolymer composition enhanced the circulation time of CPT in the blood stream, which will contribute to recruitment to solid tumor sites.

2. Materials and methods

2.1. Materials

Poly(ethylene glycol)–poly(β-benzyl L-aspartate) block copolymer (PEG–PBLA) was synthesized as described previously (Yokoyama et al., 1992). (s)-(+)-CPT was purchased from Aldrich Chem. Co. (Milw., WI, USA). 1,8-Diazabicyclo[5,4,0]7-undecene (DBU), high performance liquid chromatography (HPLC) grade acetonitrile and triethylamine acetate were purchased from Wako Pure Chemicals, (Tokyo, Japan). *N*,*N*-dimethylformamide (DMF) was dried over a molecular sieve (4A), and distilled under reduced pressure. Other chemicals were of reagent grade.

2.2. Synthesis of diblock copolymers (PEG–PBLA and its derivatives)

Poly(ethylene glycol)–poly(β-benzyl L-aspartate) block copolymer (PEG–PBLA) was synthesized by ring-opening polymerization of benzyl L-aspartate *N*-carboxy anhydride from a terminal primary amino group of α-methyl-ω-amino-poly(oxyethylene), and poly(ethylene glycol)–poly(aspartic acid) block copolymer (PEG-P(Asp)) was obtained by alkaline hydrolysis of PEG–PBLA as reported previously (Yokoyama et al., 1992). Briefly, PEG–PBLA was dispersed in a measured volume of 0.5N NaOH that contained 1.5 mol. equivalents of NaOH to the benzyl aspartate residue of PEG–PBLA. With stirring at room temperature, the solution became homogeneous in approximately 15 min. Then, 6N HCl was added (10 mol. equivalents of HCl to the benzyl aspartate residue) to the solution, and this solution was dialyzed against 0.1N HCl, followed by distilled water using a SpectraPor®-6 dialysis membrane (MWCO: 1000). PEG-P(Asp) block copolymer was obtained by freeze-drying the dialyzed solution.

Esterification of the aspartic acid residues was achieved through nucleophilic substitution of the carboxyl group with a halogen compound using 1,8-diazabicyclo [5,4,0] 7-undecene (DBU) as a catalyst, as reported previously (Opanasopit et al., 2004). PEG-P(Asp) block copolymer was dissolved in DMF and added to a halogen compound or a mixture of two halogen compounds (benzyl bromide, *n*-butyl bromide, or lauryl bromide) and DBU. The reaction mixture was stirred at 50 °C for ca. 16 h. Then, it was poured into a 10-fold volume excess of diethyl ether, and the precipitated polymer was collected by filtration, followed by washing with diethyl ether and drying. In order to remove DBU from the polymer products, polymers were dissolved in DMSO and added to 6N HCl that was much excess equivalents to the aspartic acid residue of the block copolymer. Then, this solution was dialyzed against distilled water, and freeze-dried.

Ester contents of the block copolymers were determined in ^{1}H NMR spectra by comparing the methylene protons of the hydrophilic PEG block and protons of the hydrophobic moieties of the poly(aspartate) block.

2.3. Preparation of CPT-loaded micelles and CPT solution

CPT was incorporated into polymeric micelles by an evaporation method as reported previously (Opanasopit et al., 2004). Briefly, CPT (0.05, 0.1, 0.2, or 0.4 (CPT/polymer, w/w)) was

dissolved in a mixture of chloroform (1 ml per 1 mg CPT) and acetonitrile (0.67 ml per 1 mg CPT), and added to 5 mg of block copolymer. The solvent was removed by evaporation in a nitrogen gas flow. Then, 3 ml of distilled water was added and sonicated for 2 min using a probe type sonicator model VC 100 (Sonics & Materials Inc., Newtown, Connecticut, USA) equipped with a standard 6 mm probe in a cycle of sonication for 0.5 s and standby for 0.5 s at 80 °C. The solution obtained was centrifuged at 1400 × *g* for 10 min. Subsequently, the supernatant was collected and filtered through a 1 μm pore-sized nylon filter (Puradisc 25NYL, 6751-2510, Whatman, Clifton, New Jersey, USA). CPT-loaded polymeric micelles were kept in a freezer at −20 °C until animal experiments.

The CPT solution was prepared by dissolving CPT (13 mg) in 50 ml of polyethylene glycol 400, propylene glycol and polysorbate 80 (40:50:2, volume ratio) (Yang et al., 1999).

2.4. Determination of CPT content and particle size of micelles

CPT-loaded micelles were dissolved in a mixture of DMSO:H_2O (9:1). The amount of CPT incorporated into polymeric micelles was determined by UV–vis absorption at 365 nm. The incorporation efficiency was calculated as the percentage share of the initial drug used in the preparation for incorporation into the micelles. The mean particle diameters were determined using a dynamic light scattering particle size analyzer (DLS-7000, Otsuka Electronics, Osaka, Japan) at 25 °C by diluting dispersion to an appropriate volume with water.

2.5. Incorporation stability of CPT-loaded micelles evaluated by GPC

The incorporation stability of CPT-loaded micelles was evaluated by gel-permeation chromatography (GPC) as described previously (Yokoyama et al., 1994). GPC was carried out using a Tosoh HPLC system SC-8010 equipped with a Tosoh TSKgel G3000PW_{XL} column. Distilled water was used as the eluent at a flow rate of 1 ml/min at 40 °C. Sample solutions (50 μl) were injected into the column. The detection was performed by measuring absorption at 351 nm for CPT using a Tosoh UV-8010 detector and a refractive index (RI) detector for polymers. A micelle peak was observed at the gel-exclusion volume. GPC with UV detection allowed us to evaluate the nature of the polymeric micelles obtained and the degree of drug incorporation. The peak area detected by UV absorption represents the amount of CPT loaded into the micelles. Therefore, the ratio of the micelle peak area/CPT concentration of the injected sample [CPT] was evaluated as the incorporation stability of CPT-loaded micelles. The small values of the peak area/[CPT] means that most of the CPT was adsorbed to the GPC column by hydrophobic interactions due to unstable packaging of CPT in the micelles. When this ratio was large, CPT was more stably incorporated into micelles.

2.6. Measurement of CPT concentration in plasma

CPT-loaded micelles were intravenously (i.v.) administered to male ddY mice (weighing 18–20 g, Tokyo Laboratory Animal Science Co., Ltd., Tokyo, Japan) via lateral tail veins at a dose of 2.5 mg/kg. For each sampling point, three mice were injected with CPT-loaded micelles. At various time points after the administration, approximately 1 ml of blood was withdrawn using a heparinized syringe and centrifuged at 15,300 × *g* for 4 min to obtain the plasma. Immediately after that, 0.15 M aqueous phosphoric acid was added to the plasma and mixed vigorously (Onishi et al., 2003). CPT was extracted with chloroform: methanol (4:1 volume ratio). After centrifugation of the mixture at 15,300 × *g* for 4 min, 25 μl of the chloroform: methanol layer was directly injected into the HPLC system to determine the concentration of CPT. This operation gave the total concentration of free and incorporated CPT in micelles.

The HPLC analysis was performed at room temperature. A Shimadzu LC-10AT (Shimadzu Corp., Japan) apparatus equipped with a Shimadzu RF-$10A_{XL}$ fluorescence detector in which the excitation and emission wavelength was set at 369 and 426 nm, respectively, was used. A Tosoh TSK-gel ODS-80Ts column (150 mm × 4.6 mm i.d.) was also used. The mobile phase was composed of 23:77 (v/v) acetonitrile–triethylamine acetate buffer (1% (v/v) adjusted to pH 5.5 with glacial acetic acid), and the flow rate was set at 1 ml/min (Warner and Burke, 1997). The areas under the concentration curve (from 0 to 24 h; AUC) were calculated using the trapezoid method.

2.7. Statistical analysis

The results were analyzed statistically using the Student's *t*-test. When comparisons between groups yielded a value for $P < 0.05$, the difference between those groups was considered significant.

3. Results and discussion

3.1. Characterization

Polymeric micelles with a particle diameter of less than 100 nm and a PEG-coated surface have been found to well avoid entrapment by the reticuloendothelial system (RES) and to well leak in diseased areas with highly permeable blood vessels, resulting in passive targeting to the diseased sites (Yokoyama et al., 1993; Kwon et al., 1994); this is known as the EPR effect. In order to sufficiently acquire this EPR effect, we examined the effect of various polymers on the CPT incorporation stability and evaluated the pharmacokinetic profile of CPT-loaded micelles.

Chemical structure of poly(ethylene glycol)–poly(aspartate ester) block copolymer (PEG-P(Asp(R))) is shown in Fig. 2. The block copolymers are coded by the chain lengths of both blocks, the name of the hydrophobic group, and the degree of esterification as summarized in Table 1. For example, 5-27 Bz44 represents a block copolymer composed of a PEG block of molecular weight 5000 and a P(Asp) block possessing 27 units of aspartic acid, in which 44%

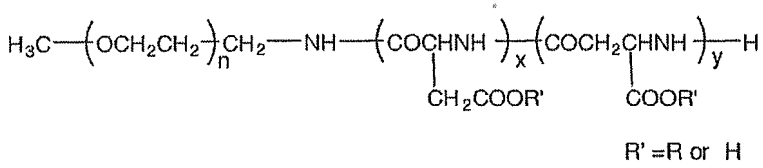

Fig. 2. Chemical structure of poly(ethylene glycol)–poly(aspartate ester) block copolymer (PEG-P(Asp(R))).

Table 1
Poly(ethylene glycol)–poly(aspartate ester) diblock copolymers (PEG-P(Asp(R)))

Code	PEG (MW)	Asp[a] ester ($x+y$ unit)	Ester (R)	Esterification (%)
5-27 Bz44	5000	27.1	Benzyl	44
5-27 Bz57	5000	27.1	Benzyl	57
5-27 Bz75	5000	27.1	Benzyl	75
5-52 Bz74	5000	52.0	Benzyl	74
12-25 Bz71	12000	27.1	Benzyl	71
12-50 Bz63	12000	50.0	Benzyl	63
5-27 *n*-Bu6 + Bz57	5000	27.1	*n*-Butyl + benzyl	6 + 57
5-27 Lau5 + Bz58	5000	27.1	Lauryl + benzyl	5 + 58

[a] Asp: aspartate.

of the aspartic acid residues are esterified with a benzyl group.

3.2. Ester groups of polymers

To determine the structural requirements for stability, polymers with three kinds of ester groups were synthesized. The incorporation of CPT into polymeric micelles was successfully achieved by the evaporation method which provided high CPT yields (Opanasopit et al., 2004). Table 2 shows the effect of ester groups (benzyl and mixture (benzyl + lauryl, benzyl + *n*-butyl)) on the entrapment efficiency, incorporation stability evaluated by GPC and the % injected dose in plasma after 4 h. When the ratio of micelles peak area/CPT concentration [CPT] was large, the CPT incorporated into the micelles was more stable. CPT micelles of these three ester groups showed similar stability in vitro, but not in vivo. Benzyl polymeric micelles suggested a longer circulation time than *n*-butyl and lauryl ones in spite that the mixture had a more hydrophobic inner core than benzyl. This implies that not only hydrophobicity but also physical factors such as rigidity and π–π interactions of the inner core-forming block contributed to the incorporation, since the lauryl ester (C12) is more hydrophobic than the benzyl ester (C7).

Table 3
Effect of PEG length (5000 or 12,000) and Asp unit (27 or 50) on stability of CPT-loaded micelles at a feeding ratio (CPT/polymer) of 0.4 (w/w)

Code	Peak area/[CPT][a]	% Injected dose in plasma after 4 h[b]
5-27 Bz75	46.5	9.3 ± 1.8
12-25 Bz71	26.5	2.6 ± 0.6
5-52 Bz74	86.1	6.7 ± 0.5
12-50 Bz63	21.9	2.2 ± 0.4
CPT-solution[c]	–[d]	0.04 ± 0.03

[a] Incorporation stability; peak area, evaluated by GPC, was divided by CPT concentration in micelles [CPT] (n = 1–2).
[b] Results at a dose of 2.5 mg/kg are given as the mean ± S.D. (n = 3).
[c] CPT was dissolved in polyethylene glycol 400:propylene glycol: Tween 80 = 40:58:2 (volume ratio).
[d] Not done.

PEG–PBLA can be handled as benzyl-100% because its aspartic acid residues were fully benzylated. However, in the stability assay using GPC, PEG–PBLA micelles provided much lower incorporation stability than the benzyl-57% block copolymer. This indicates that the conformation and/or configuration of the hydrophobic inner core-forming polymer block contributes to a stable incorporation by providing the appropriate space for CPT.

3.3. PEG length and Asp unit of polymers

To determine the contribution of PEG length and Asp unit to the micelles' stability, four polymeric micelles of Bz with different combinations of PEG length (5000 or 12,000) and Asp units (27 and 50) were prepared (Table 3). Compared with the CPT solution as a control, at both 27 and 50 Asp units, CPT micelles of PEG 5000 showed a longer circulation than those of PEG 12,000 in vivo.

An increase in the chain length of a hydrophobic block at a given chain length of a hydrophilic block causes a decrease in the critical micelle concentration (CMC) (Leibler et al., 1983). In contrast, the ADR-loaded PEG-P(Asp(ADR)) micelles, pos-

Table 2
Effect of ester group of polymer 5-27 (PEG 5000-Asp unit 27) on stability of CPT-loaded micelles at a feeding ratio (CPT/polymer) of 0.1 (w/w)

Code	Esterification (%) of diblock copolymer	Entrapment efficiency (%)[a]	Peak area/[CPT][b]	% Injected dose in plasma after 4 h[c]
5-27 *n*-Bu6 + Bz57	*n*-Bu 6 + Bz57	37.8	58.1	0.15 ± 0.08
5-27 Lau5 + Bz58	Lauryl 5 + Bz58	47.5	48.3	0.07 ± 0.03
5-27 Bz57	Bz57	88.6	55.3	7.6 ± 0.8
PEG–PBLA	Bz100	67.7	1.5	–[d]

[a] n = 1–2.
[b] Incorporation stability; peak area, evaluated by GPC, was divided by CPT concentration in micelles [CPT] (n = 1–2).
[c] Results at a dose of 2.5 mg/kg are given as the mean ± S.D. (n = 3).
[d] Not done.

sessing a longer hydrophilic PEG chain and a shorter hydrophobic P(Asp(ADR)) chain circulated longer in blood (Kwon et al., 1993, 1994), accumulated more in tumors (Kwon et al., 1994), and showed greater antitumor activity (Yokoyama et al., 1993). This is a reversed relationship estimated from the CMC phenomenon of block copolymers. This implies that dynamic stability of the polymeric micelles that is defined with a dissociation constant of the micelle structure is more important in vivo than static micelle stability that is defined with CMC values. In this study, at a similar number of the Asp units, the micelles possessing PEG 5000 was found to be more stable than those possessing PEG 12,000 in blood circulation. This fact was opposite to the ADR case. More detailed study is required to elucidate the relationship between in vivo stability and compositions of polymeric micelles by more quantitatively evaluating strength and nature (e.g., degree of contribution of π–π interaction) of interactions utilized for micelle formation and drug incorporation.

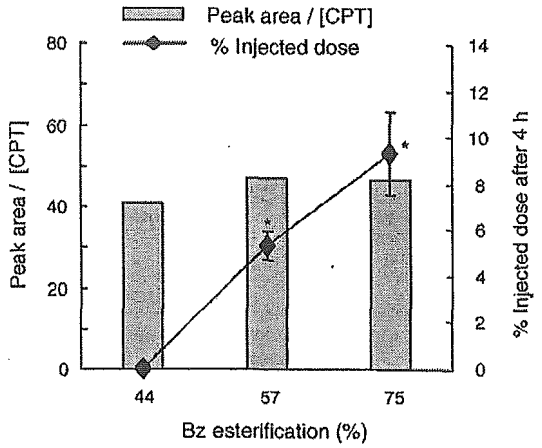

Fig. 3. Effect of esterification of 5-27 Bz on stability of CPT-loaded micelles at a feeding ratio (CPT/polymer) of 0.4 (w/w). The ratio of peak area/[CPT] indicated the incorporation stability of CPT-loaded micelles. Percentage injected dose represents the mean ± S.D., $n=3$. $^{*}P<0.05$; compared with 5-27 Bz44.

3.4. Benzyl ester content in micelles

For the ADR-loaded polymeric micelle system, a larger amount of the chemically conjugated ADR (63 mol% with respect to the aspartic acid residue of the block copolymer) provided more stable circulation in blood of the physically entrapped ADR that exhibited targeted anti-tumor activity than a smaller amount case (41 mol%). In the present study, to determine the contribution of esterification to micelle stability, three kinds of 5-27 micelles with different amounts of Bz were prepared. The mean particle sizes of 5-27 Bz44, Bz57 and Bz75 were 275.8, 182.7 and 196.1 nm, respectively. The effect of esterification of 5-27 Bz on the stability of CPT-loaded micelles at a feeding ratio (CPT/polymer) of 0.4 (w/w) was examined by GPC and by measuring the % injected dose in plasma after 4 h (Fig. 3). When the benzyl ester content was increased from 44 to 75%, the stability of polymeric micelles was similar in vitro, but CPT-loaded micelles of 5-27 Bz44 showed poor circulation stability. CPT-loaded micelles were able to maintain stability in vivo on esterification of more than 57% of the polymer. As showing Table 2, PEG–PBLA (Bz100%) micelles were not stable in in vitro. Therefore, stable micelle formulation was obtained when the esterification ratio of Bz was appropriate (57–75%). This finding corresponded well that CPT release rate from the micelles for PEG–PBLA or 5-27 Bz44 was faster than that for 5-27 Bz75, when incubated in PBS at 37 °C (Opanasopit et al., 2004). The result suggested that the contribution of π–π interaction between aromatic groups of CPT molecules could be maintained, when the degree of esterification of Bz was more than 57%.

3.5. Feeding ratio of CPT/polymer in micelle

To investigate the influence of feeding ratio on the micelle characteristics, CPT-loaded polymeric micelles were prepared at the different feeding ratio (0.05, 0.1, 0.2 and 0.4 (w/w)). Fig. 4 shows the entrapment efficiency, mean particle size, and the incorporation and circulation stability of CPT-loaded 5-27 Bz57 polymeric micelles, respectively. Regardless of feeding

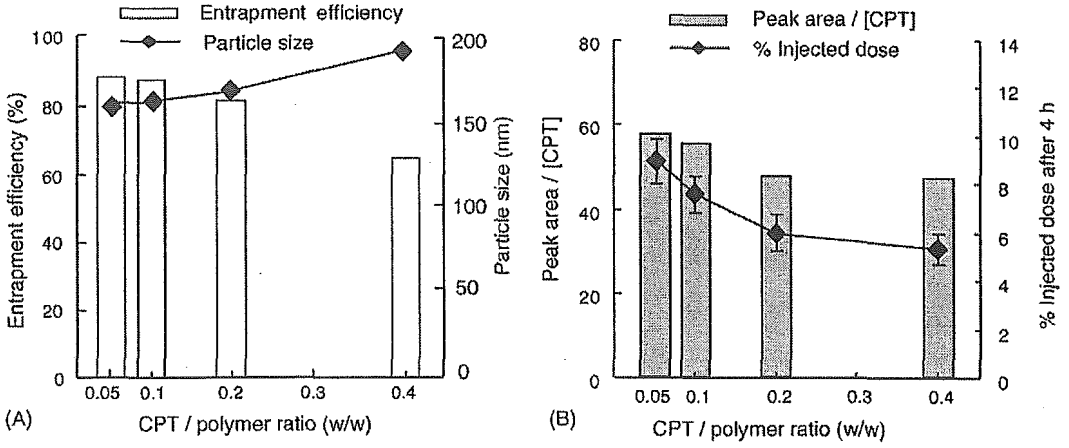

Fig. 4. Effect of feeding ratio (CPT/5-27 Bz57 polymer, w/w) on entrapment efficiency, particle size (A), and the incorporation (peak area/[CPT]) and circulation stability of CPT-loaded micelles (B). Particle size and % injected dose represent the mean ± S.D., $n=3$.

ratio of CPT/polymer, obtained CPT-loaded micelles showed similar particle size (150–200 nm) and stability of in vitro and in vivo (5–10% injected dose after 4 h). CPT-loaded 5-27 Bz57 micelles were stable in vivo even if the amount of CPT in the polymer was increased. In the case of ADR-loaded polymeric micelles, 21 w/w% ADR was physically incorporated whereas intact ADR, having antitumor activity, accounted for only 5 w/w% (Yokoyama et al., 1999). The feeding ratio of 0.4 (w/w) CPT/polymers corresponds to more than 20 w/w% of CPT in obtained micelles, where CPT was incorporated in the active lactone form (>95%). Therefore, this system will be able to deliver a massive amount of intact drug to the targeted site.

3.6. Plasma concentration–time profiles

As a stable formulation of CPT-loaded micelle was obtained using the polymer with 57–75% Bz esterification at a feeding ratio (CPT/polymer) of 0.4 (w/w), the plasma pharmacokinetics of the CPT-loaded 5-27 Bz63 polymeric micelles was compared with unstable formulations such as 5-27 Bz44 and CPT solution (Fig. 5). CPT-loaded 5-27 Bz63 and 5-27 Bz44 micelles at a feeding ratio (CPT/polymer) of 0.4 (w/w) showed 275.8 ± 14.8 and 276.5 ± 24.8 nm in size, respectively. As expected from Fig. 3, a long-circulation was obvious for the CPT in 5-27 Bz63 compared to 5-27 Bz44 and CPT solution. This finding corresponded with the result of CPT release from polymeric micelles in vitro, showing the slower CPT release from 5-27 Bz75 than 5-27 Bz44 in PBS at 37 °C (Opanasopit et al., 2004). Hydrophilic PEG chains exposed to the aqueous surroundings may prevent the adsorption of blood proteins onto the micelles' surface and from being cleared through RES. In spite of similar particle size, the stable polymeric micelle (Bz63) showed about a 17-fold lower clearance value than the unstable one (Bz44) (Table 4). This finding suggested that the stable incorporation of CPT into micelles by the hydrophobic interaction of intact CPT with inner core of polymeric micelles, e.g., π–π interactions of the benzyl ester, may be important in the circulation stability.

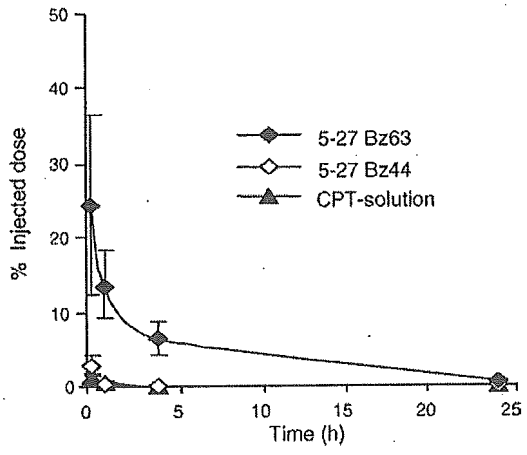

Fig. 5. Plasma concentration–time curves of the CPT-loaded 5-27 Bz (44 or 63) micelles and CPT solution following i.v. administration at a dose of 2.5 mg CPT/kg in ddY mice. The feeding ratio (CPT/polymer) was 0.4 (w/w). Results are given as the mean ± S.D., $n=3$.

Table 4
Pharmacokinetic parameters after i.v. administration of CPT-loaded 5-27 Bz (44 or 63) micelles in mice at a dose of 2.5 mg/kg

Code	AUC (μg h ml^{-1})	Clearance (ml h^{-1} g^{-1})	
5-27 Bz63	47.0 ± 2.4	0.053 ± 0.003	**
5-27 Bz44	2.7 ± 0.02	0.91 ± 0.007	

The feeding ratio (CPT/polymer) was 0.4 (w/w). AUC: area under the concentration–time curve from 0 to 24 h. Results are given as the mean±S.D. ($n=3$).
** $P<0.01$

4. Conclusion

The stable formulation of CPT-loaded micelles in vivo strongly depended on the amount of benzyl esters and length of the PEG of polymers, more so than in vitro. A stable formulation of CPT-loaded micelles was obtained using PEG-P(Asp) with a PEG of 5000 (MW), 27 Asp units, and 57–75% benzyl esterification. The CPT-loaded micelles are potentially delivered to tumor sites owing to an extended circulation in the blood stream.

Acknowledgments

We are grateful to Ms. C. Kanai, Ms. S. Katayama and Ms. C. Fujita for their technical assistance.

References

Burke, T.G., Staubus, A.E., Mishra, A.K., 1992. Liposomal stabilization of camptothecin's lactone ring. J. Am. Chem. Soc. 114, 8318–8319.
Cortesi, R., Esposito, E., Maietti, A., Menegatti, E., Nastruzzi, C., 1997. Formulation study for the antitumor drug camptothecin: liposomes, micellar solution, and a microemulusion. Int. J. Pharm. 159, 95–103.
Fassberg, J., Stella, V.J., 1992. A kinetic and mechanistic study of the hydrolysis of camptothecin and some analogues. J. Pharm. Sci. 81, 676–684.
Giovanella, B.C., Hinz, H.R., Kozielski, A.J., Stehlin Jr., J.S., Silber, R., Potmesil, M., 1991. Complete growth inhibition of human cancer xenografts in nude mice by treatment with 20-(*S*)-camptothecin. Cancer Res. 51, 3052–3055.
Giovanella, B.C., Stehlin, J.S., Wall, M.E., Wani, M.C., Nicholas, A.W., Liu, L.F., Silber, R., Potmesil, M., 1989. DNA topoisomerase I-targeted chemotherapy of human colon cancer in xenografts. Science 246, 1046–1048.
Hertzberg, R.P., Caranfa, M.J., Hecht, S.M., 1989. On the mechanism of topoisomerase I inhibition by camptothecin: evidence for binding to an enzyme-DNA complex. Biochemistry 28, 4629–4638.
Kang, J., Kumar, V., Yang, D., Chowdhury, P.R., Hohl, R.J., 2002. Cyclodextrin complexation: influence on the solubility, stability, and cytotoxicity of camptothecin, an antineoplastic agent. Eur. J. Pharm. Sci. 15, 163–170.
Kwon, G., Suwa, S., Yokoyama, M., Okano, T., Sakurai, Y., Kataoka, K., 1994. Enhanced tumor accumulation and prolonged circulation times of micelle-forming poly(ethylene oxide-aspartate) block copolymer-adriamycin conjugates. J. Control. Rel. 29, 17–23.
Kwon, G.S., Yokoyama, M., Okano, T., Sakurai, Y., Kataoka, K., 1993. Biodistribution of micelle-forming polymer-drug conjugates. Pharm. Res. 10, 970–974.
Leibler, L., Orland, H., Wheeler, J.C., 1983. Theory of critical micelle concentration for solutions of block copolymers. J. Chem. Phys. 79, 3550–3557.
Maeda, H., 2000. The enhanced permeability and retention (EPR) effect in tumor vasculature. The key role of tumor-selective macromolecular drug targeting. Adv. Enzyme Regul. 41, 189–207.

Maeda, H., Wu, J., Sawa, T., Matsumura, Y., Hori, K., 2000. Tumor vascular permeability and the EPR effect in macromolecular therapeutics: a review. J. Control. Rel. 65, 271–284.

Matsumura, Y., Maeda, H., 1986. A new concept for macromolecular therapeutics in cancer chemotherapy: mechanism of tumoritropic accumulation of proteins and the antitumor agent smancs. Cancer Res. 46, 6387–6392.

Moertel, C.G., Schutt, A.J., Reitemeier, R.J., Hahn, R.G., 1972. Phase II study of camptothecin (NSC-100880) in the treatment of advanced gastrointestinal cancer. Cancer Chemother. Rep. 56, 95–101.

Onishi, H., Machida, Y., Machida, Y., 2003. Antitumor properties of irinotecan-containing nanoparticles prepared using poly(DL-lactic acid) and poly(ethylene glycol)-block-poly(propylene glycol)-block-poly(ethylene glycol). Biol. Pharm. Bull. 26, 116–119.

Opanasopit, P., Yokoyama, M., Watanabe, M., Kawano, K., Maitani, Y., Okano, T., 2004. Block copolymer design for camptothecin incorporation into polymeric micelles for passive tumor targeting. Pharm. Res. 21, 2001–2008.

Shenderova, A., Burke, T.G., Schwendeman, S.P., 1999. The acidic microclimate in poly(lactide-co-glycolide) microspheres stabilizes camptothecins. Pharm. Res. 16, 241–248.

Singer, J.W., Bhatt, R., Tulinsky, J., Buhler, K.R., Heasley, E., Klein, P., de Vries, P., 2001. Water-soluble poly-(L-glutamic acid)-Gly-camptothecin conjugates enhance camptothecin stability and efficacy in vivo. J. Control. Rel. 74, 243–247.

Tong, W., Wang, L., D'Souza, M.J., 2003. Evaluation of PLGA microspheres as delivery system for antitumor agent-camptothecin. Drug Dev. Ind. Pharm. 29, 745–756.

Wall, M.E., Wani, M.C., 1995. Camptothecin and analogs: from discovery to clinic. In: Potmesil, M., Pinedo, H. (Eds.), Camptothecin: New Anticancer Agents. CRC Press, Boca Raton, FL, pp. 21–41.

Wall, M.E., Wani, M.C., Cook, C.E., Palmer, K.H., Mcphail, A.T., Sim, G.A., 1966. Plant antitumor agents. I. The isolation and structure of camptothecin, a novel alkaloidal leukemia and tumor inhibitor from Camptotheca acuminate. J. Am. Chem. Soc. 88, 3888–3890.

Warner, D.L., Burke, T.G., 1997. Simple and versatile high-performance liquid chromatographic method for the simultaneous quantitation of the lactone and carboxylate forms of camptothecin anticancer drugs. J. Chromatogr. B: Biomed. Sci. Appl. 691, 161–171.

Yang, S.C., Lu, L.F., Cai, Y., Zhu, J.B., Liang, B.W., Yang, C.Z., 1999. Body distribution in mice of intravenously injected camptothecin solid lipid nanoparticles and targeting effect on brain. J. Control. Rel. 59, 299–307.

Yokoyama, M., Fukushima, S., Uehara, R., Okamoto, K., Kataoka, K., Sakurai, Y., Okano, T., 1998. Characterization of physical entrapment and chemical conjugation of adriamycin in polymeric micelles and their design for in vivo delivery to a solid tumor. J. Control. Rel. 50, 79–92.

Yokoyama, M., Inoue, S., Kataoka, K., Yui, N., Sakurai, Y., 1987. Preparation of adriamycin-conjugated poly(ethylene glycol)-poly(aspartic acid) block copolymer. A new type of polymeric anticancer agent. Die Makromolekulare Chemie Rapid Commun. 8, 431–435.

Yokoyama, M., Kwon, G.S., Okano, T., Sakurai, Y., Seto, T., Kataoka, K., 1992. Preparation of micelle-forming polymer-drug conjugates. Bioconjug. Chem. 3, 295–301.

Yokoyama, M., Kwon, G.S., Okano, T., Sakurai, Y., Ekimoto, H., Okamoto, K., Mashiba, H., Seto, T., Kataoka, K., 1993. Composition-dependent in vivo antitumor activity of adriamycin-conjugated polymeric micelle against murine colon adenocarcinoma 26. Drug Del. 4, 11–19.

Yokoyama, M., Kwon, G.S., Okano, T., Sakurai, Y., Naito, M., Kataoka, K., 1994. Influencing factors on in vitro micelle stability of adriamycin-block copolymer conjugates. J. Control. Rel. 28, 59–65.

Yokoyama, M., Miyauchi, M., Yamada, N., Okano, T., Sakurai, Y., Kataoka, K., Inoue, S., 1990. Characterization and anticancer activity of the micelle-forming polymeric anticancer drug adriamycin-conjugated poly(ethylene glycol)–poly(aspartic acid) block copolymer. Cancer Res. 50, 1693–1700.

Yokoyama, M., Okano, T., Sakurai, Y., Ekimoto, H., Shibazaki, C., Kataoka, K., 1991. Toxicity and antitumor activity against solid tumors of micelle-forming polymeric anticancer drug and its extremely long circulation in blood. Cancer Res. 51, 3229–3236.

Yokoyama, M., Okano, T., Sakurai, Y., Fukushima, S., Okamoto, K., Kataoka, K., 1999. Selective delivery of adriamycin to a solid tumor using a polymeric micelle carrier system. J. Drug Target. 7, 171–186.

Yokoyama, M., Opanasopit, P., Okano, T., Kawano, K., Maitani, Y., 2004. Polymer design and incorporation methods for polymeric micelle carrier system containing water-insoluble anti-cancer agent camptothecin. J. Drug Target., 373–384.

Zamai, M., VandeVen, M., Farao, M., Gratton, E., Ghiglieri, A., Castelli, M.G., Fontana, E., D'Argy, R., Fiorino, A., Pesenti, E., Suarato, A., Caiolfa, V.R., 2003. Camptothecin poly[*n*-(2-hydroxypropyl) methacrylamide] copolymers in antitopoisomerase-I tumor therapy: intratumor release and antitumor efficacy. Mol. Cancer Ther. 2, 29–40.

Available online at www.sciencedirect.com
SCIENCE DIRECT®
ELSEVIER
International Journal of Pharmaceutics 300 (2005) 38–47
international journal of pharmaceutics
www.elsevier.com/locate/ijpharm

Cholesteryl hemisuccinate as a membrane stabilizer in dipalmitoylphosphatidylcholine liposomes containing saikosaponin-d

Wu-xiao Ding [a], Xian-rong Qi [a,*], Ping Li [b], Yoshie Maitani [c], Tsuneji Nagai [c]

[a] *Department of Pharmaceutics, School of Pharmaceutical Sciences, Peking University, Beijing 100083, China*
[b] *Department of Materia Medica and Pharmacology, China–Japan Friendship Hospital, Beijing 100029, China*
[c] *Institute of Medicinal Chemistry, Hoshi University, Shinagawa-Ku, Tokyo 142-8501, Japan*

Received 25 February 2005; received in revised form 12 April 2005; accepted 10 May 2005
Available online 22 June 2005

Abstract

In the present study, cholesteryl hemisuccinate (CHEMS) was evaluated for use as a membrane stabilizer in dipalmitoylphosphatidylcholine (DPPC) liposomes. Differential scanning calorimetry (DSC) and a calcein release study showed that CHEMS was more effective than cholesterol (CHOL) in increasing DPPC membrane stability. The findings of Fourier transform infrared spectroscopy (FT-IR) also suggested that CHEMS interacts with DPPC via both hydrogen bonding and electrostatic interaction. More importantly, CHEMS did not interact with saikosaponin-d (SSD), a triterpene saponin from Bupleurum species, unlike CHOL. SSD-containing liposomes with DPPC, CHEMS and DSPE-PEG could greatly decrease the hemolytic activity of SSD. This study demonstrated that CHEMS has more stabilization ability than CHOL since CHEMS may exhibit both hydrogen bond interaction and electrostatic interaction with DPPC membrane while CHOL only has hydrogen bond interaction, resulting in stable and low-hemolytic SSD-liposomes.
© 2005 Elsevier B.V. All rights reserved.

Keywords: Cholesteryl hemisuccinate; Saikosaponin-d; Saponin; Liposome; Differential scanning calorimetry; Fourier transform infrared spectroscopy

1. Introduction

Saikosaponin-d (SSD) (Fig. 1A), a triterpene saponin from Bupleurum species, has shown corticosterone-like activity (Yokoyama et al., 1984), Na^+-, K^+-ATPase inhibiting action (Zhou et al., 1996), immunoregulatory action (Ushio and Abe, 1991) and anti-platelet activating factor activity (Nakamura et al.,

Abbreviations: DPPC, dipalmitoylphosphatidylcholine; CHEMS, cholesteryl hemisuccinate; CHOL, cholesterol; SSD, saikosaponin-d; DSPE-PEG, methoxypolyethyeneglycol (Mr2000)-distearoylphosphatidylethanolamine; DSC, differential scanning calorimetry; FT-IR, Fourier transform infrared spectroscopy

* Corresponding author. Tel.: +86 10 82801584; fax: +86 10 82802791.
E-mail address: qixr2001@yahoo.com.cn (X.-r. Qi).

0378-5173/$ – see front matter © 2005 Elsevier B.V. All rights reserved.
doi:10.1016/j.ijpharm.2005.05.005

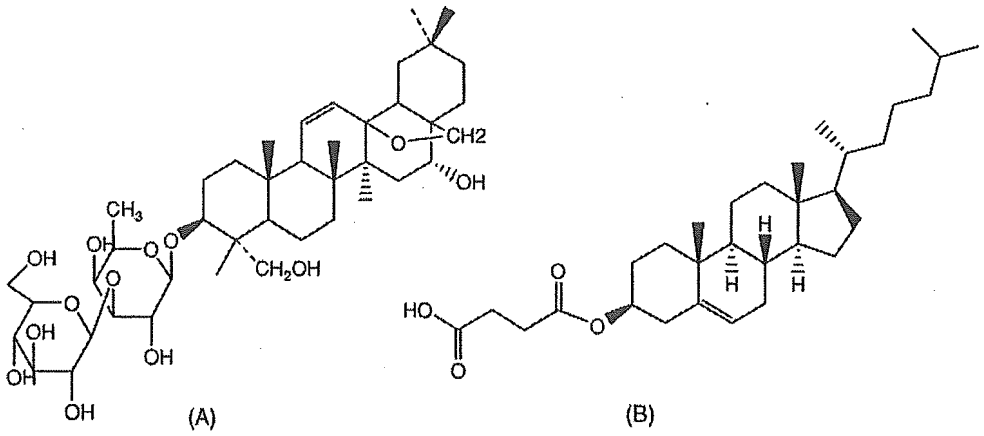

Fig. 1. Structures of saikosaponin-d (A) and cholesteryl hemisuccinate (B).

1993). It has been widely studied as a potential medication in the treatment of nephritis, nephrosis syndrome (Abe et al., 1986) and hepatic fibrosis (Cheng et al., 1999). Furthermore, bupleurum soup and particles for oral administration, the main active constituent of which is SSD, have achieved great success in the treatment of chronic glomerulonephritis and glomerulosclerosis (Zhang, 1993; Cheng, 1994).

SSD and other saikosaponins given in oral dosage form are not readily absorbed in the gastrointestinal tract and easily metabolized by glycosidase to less potent prosaikogenins before absorption occurs (Kida et al., 1998), leading to a dose of 200–300 mg and the need for treatment three times per day for adults. Therefore, the low level (less than 0.01%) of saikosaponins in Bupleurum species and their tendency to transform during separation and purification (Wen, 1993) hinder practical application in the clinic.

Other routes such as intraperitoneal and intramuscular administration have also been explored and are thought to enhance the corticosterone level in serum (Yokoyama et al., 1984; Zhong et al., 1993), however the risk of hemolysis should also be carefully considered. It is widely recognized that the hemolytic activity of SSD is caused by its complex with cholesterol (CHOL) on erythrocyte membrane, leading to membrane disruption and cell lysis. Driven by the need to reduce the hemolytic activity and make possible injections with less SSD, the liposome was chosen as a carrier for the present research because of its non-toxic, enhanced therapeutic efficacy and reduction of drug toxicity (Gregoriads, 1988).

It has been mentioned (Wang, 1992) that sterols with C_3-β-OH (including CHOL) form an insoluble complex with SSD, but, sterols with C_3-α-OH and esterified or glycosidated at C_3-OH do not. It is difficult to prepare liposomes containing SSD (SSD-liposomes), since SSD will form an insoluble complex with CHOL, which is routinely used to stabilize liposomes. Therefore, there is a great need for other membrane stabilizers for the preparation of SSD-liposomes.

Cholesteryl hemisuccinate (CHEMS) (Fig. 1B) is a CHOL-derivative esterified to the 3-hydroxyl group of CHOL and is supposed not to form a complex with SSD. Until now, no toxicity profiles about CHEMS have been reported. On the other hand, it has been found to increase specific immunogenicity of tumor cells by pretreating tumor cells with CHEMS (Skornick et al., 1986). And also, CHEMS was thought to protect against acetaminophen-induced hepatocellular apoptosis (Ray et al., 1996) and carbon tetrachloride-induced hepatotoxicity. It was proved to be a powerful cytoprotective agent against carbon tetrachloride hepatotoxicity in vivo (Fariss et al., 1993). CHEMS can form pH-sensitive fusogenic vesicles when incorporated into phosphatidylethanolamine bilayers and the pH is lowered to 5.5, resulting in H-II phase formation (Ismail et al., 2000; Se'rgio et al., 2004). CHEMS has also been demonstrated to alter acyl chain motion or fluidity in cell membranes (Dumas et al., 1997; Lai et al., 1985). It was proved by fluorescence polarization to be equally effective as CHOL in reducing the acyl chain mobility of DPPC above the phase transition temperature (Massey, 1998) and reported

to be a membrane stabilizer (Zhang et al., 2000). All these attributes contribute to the suitability of CHEMS as a membrane stabilizer in the preparation of SSD-liposomes, which has not been studied in the past.

The mechanism by which CHEMS acts as a membrane stabilizer is not fully understood and little research has been done on drug-loaded liposomes using CHEMS as a membrane stabilizer. Therefore, in the present study, CHEMS was investigated for its membrane stabilization ability using DSC, calcein release and FT-IR measurements. Furthermore, the hemolytic activity of SSD-liposomes using CHEMS as a unique membrane stabilizer was evaluated.

2. Materials and methods

2.1. Materials

Dipalmitoylphosphatidylcholine (DPPC), CHOL, succinic anhydride and methoxypolyethyeneglycol (Mr 2000)-distearoylphosphatidylethanolamine (DSPE-PEG) were purchased from NOF Corporation (Japan). Saikosaponin-d (SSD, purity of 95%) was extracted from the root of *Bupleurum falcatum* by the Department of Materia Medica and Pharmacology, China–Japan Friendship Hospital. A Dialysis membrane (cutoff 8000–14,000) was purchased from Membrane Filtration Products (San Antonio, USA). All other chemicals were of reagent grade.

2.2. Synthesis of CHEMS

CHEMS was prepared according to Kuhn et al. (1975), but with 4-dimethylaminopyridine (DMAP) added as a catalyzer. The molecular weight of CHEMS determined by ESI-TOF-MS was 486.74.

2.3. DSC analysis

Liposome suspensions containing DPPC and different amounts of CHOL, CHEMS and SSD were prepared with 1/10 PBS (pH 7.4) by the film hydration and bath sonication method, with a DPPC concentration of 100 mg/ml. Ten microliters of each liposome suspension (1 mg DPPC) was transferred into a 20-μl DSC aluminum pan and subjected to DSC analysis using a DSC 2010 (Thermal Analysis, Newcastle, USA). The scan rate employed was 0.5 °C/min over the temperature range 20–50 °C, and the reference pan was filled with 1/10 PBS. The transition enthalpies (ΔH, J/g of DPPC) were calculated from the peak areas using the integration program of the TA processor, within an experimental error of ±5%.

2.4. Calcein release study

Calcein-encapsulated liposomes (DPPC-, DPPC/CHOL (10:4)-, DPPC/CHEMS (10:4)-liposomes) were prepared by the reverse phase evaporation vesicle method (Szoka and Papahadjopoulos, 1978). Briefly, 25 mg of DPPC and specific amount of CHEMS or CHOL were dissolved in 15 ml of chloroform/isopropyl ether (2:1, v/v) and mixed with 5 ml of calcein solution (1×10^{-3} mol/l in 1/10 PBS). The mixtures were sonicated by probe sonicator to give a homogeneous emulsion and then placed on a vacuum rotary evaporator until the formation of liposome suspension. The liposomes were then extruded through 200 nm-pore sized polycarbonate film at 45 °C for two times and free calcein was separated by Sephadex G-100. Calcein release from the liposomes was carried out with a dialysis method both in 1/10 PBS and in 30% rabbit plasma at 37 ± 0.5 °C.

2.5. FT-IR analysis

DPPC mixtures with CHOL, CHEMS and SSD (all with a 1:1 molar ratio) were dissolved in chloroform or a chloroform–methanol mixture for SSD. The solvent was evaporated under vacuum, the dried lipid mixture was pressed into thin KBr tablets. The tablets were scanned on a Nicolet 5DX (Thermo Electron Corp., Waltham, USA) from 400 to 4000 cm^{-1}. The separate FT-IR spectrograms were combined over the region between 1800 and 1200 cm^{-1}, which contained the band position of the P=O stretching vibration (V_s P=O), the P=O asymmetric stretching vibration (V_{as} P=O) and the asymmetry flexual vibration of the quaternary ammonium of DPPC.

2.6. Turbidity measurement

Blank liposomes (DPPC/CHOL (10:4)- and DPPC/CHEMS (10:4)-liposomes) were prepared by the film hydration and probe sonication method to

give small unilammelar vesicles (SUVs, average size, 134.6 and 102.9 nm, respectively), with the DPPC concentration at 0.5 mg/ml. An equal volume of SSD suspension of 200 μg/ml or distilled water was added to the liposome suspension, and the relative turbidity ($A_t/A_0 \times 100\%$) of liposomes was measured at 550 nm at room temperature, where A_t and A_0 represent the absorption value at time t and 0 min at 550 nm, respectively.

2.7. Hemolytic activity

SSD-liposomes with serial concentrations of SSD were prepared with DPPC, CHEMS and/or DSPE-PEG by film hydration and probe sonication. A 0.3 ml volume of SSD solution or SSD-liposomes suspension (with a lipid concentration of 2.5 mg/ml and size of about 150 nm) was put into a 5 ml glass tube, and then 2.2 ml of saline and 2.5 ml of 2% rabbit erythrocyte suspension were added. The mixtures were incubated at 37 ± 0.5 °C for 3 h and then centrifuged at 2500 rpm for 10 min. The absorption value of the supernatant was measured at 540 nm by subtracting the blank.

3. Results

3.1. Effect of CHOL, CHEMS and SSD on DPPC membrane by DSC

As illustrated in Fig. 2 and Table 1, the maximal transition temperature from gel to liquid-crystalline (T_m) and the transition enthalpy (ΔH) of the DPPC bilayer was 39.52 °C and 24.24 J/g of DPPC, respectively, addition of CHOL and CHEMS decreased the T_m value slightly and the ΔH value markedly. The T_m values of the five formulations remained at about

Table 1
The maximal transition temperature from gel to liquid-crystalline (T_m) and ΔH value of DPPC liposomes with CHOL, CHEMS and SSD (each sample contained 1 mg DPPC)

Composition (molar ratio)	T_m (°C)	ΔH (J/g of DPPC)
DPPC	39.52	24.24
DPPC:CHOL (10:2)	39.28	5.26
DPPC:CHEMS (10:2)	38.28	1.162
DPPC:CHEMS (10:1)	39.34	11.89
DPPC:SSD (10:2)	38.68	23.54

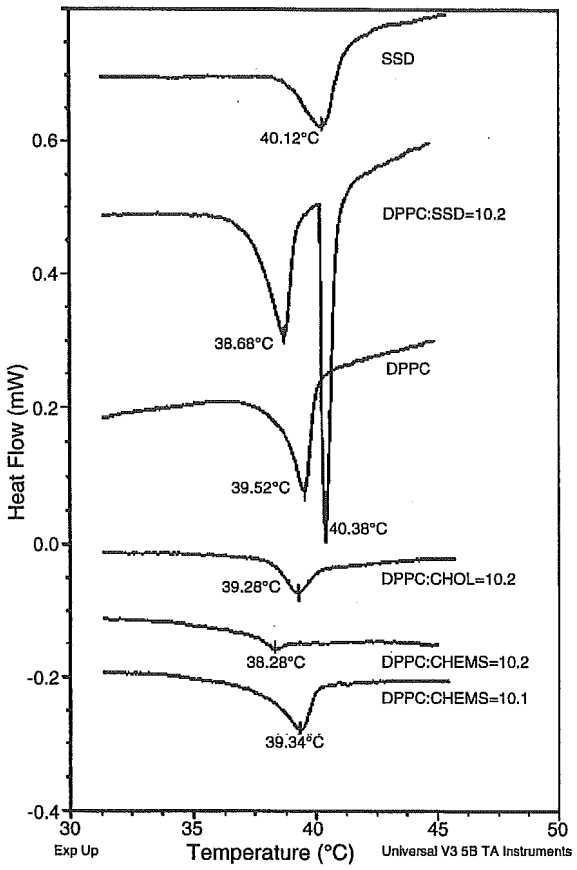

Fig. 2. DSC spectrograms of DPPC liposomes with CHEMS, CHOL and SSD.

39 °C, while the ΔH values of DPPC/CHOL (10:2)-, DPPC/CHEMS (10:1)- and DPPC/CHEMS (10:2)-liposomes were decreased markedly to 5.26, 11.89 and 1.162 J/g of DPPC, respectively.

We have found that a maximum amount of SSD that can retain in the lipid bilayers of liposomes was less 15% (SSD/total lipid, molar ratio). Therefore, in DPPC/SSD (10:2)-liposome suspension, free SSD surely existed and would form micelles after bath sonication, resulting in the second endotherm peak of 40.38 °C. The value was similar to 40.12 °C in the endotherm of SSD suspension (Fig. 2), confirming that the endotherm of 40.38 °C in DPPC/SSD (10:2)-liposome suspension was the micelles of free SSD. But the endotherm of SSD suspension was broad as compared to the sharp endotherm of 40.38 °C in DPPC/SSD (10:2)-liposome suspension, a reason may

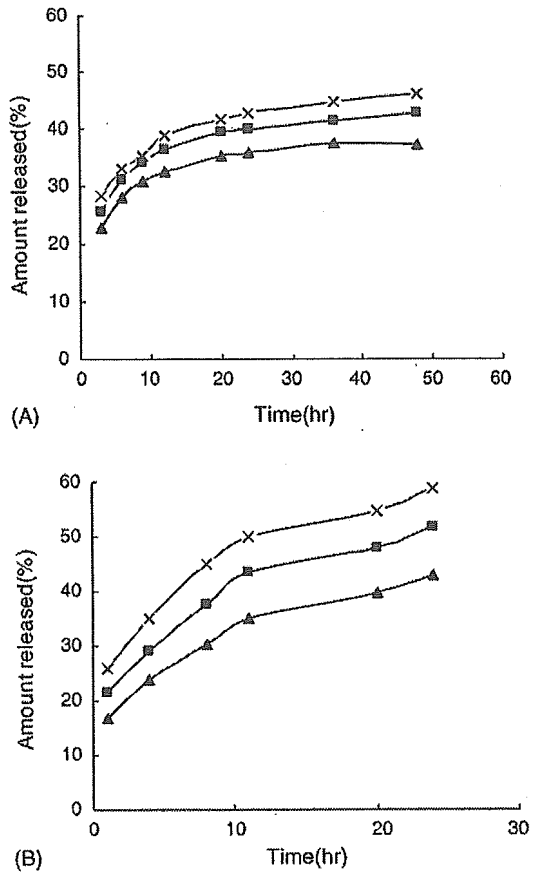

Fig. 3. Calcein release from liposomes at 37 ± 0.5 °C incubated with 1/10 PBS (A) and 30% rabbit plasma (B). (The data are means of two experiments.) (×): DPPC-liposomes, (■): DPPC/CHOL (10:4)-liposomes, (▲): DPPC/CHEMS (10:4)-liposomes.

be surmised that excessive SSD sedimentation might deposit on the base of aluminum pan, which may have interfered the heat conduction and subsequent peak appearance.

3.2. Calcein release study

Calcein release in 1/10 PBS (Fig. 3A) and in 30% rabbit plasma (Fig. 3B) were in duplicate since the experiments were parallel and the variability was very small. The results showed that the release of calcein from DPPC/CHEMS (10:4)-liposomes was slower than that of DPPC/CHOL (10:4)-liposomes, and the release in 1/10 PBS (Fig. 3A) was slower than that in 30% rabbit plasma (Fig. 3B).

3.3. Effect of CHEMS, CHOL and SSD on DPPC by FT-IR

The FT-IR spectrograms of DPPC/CHOL (1:1), DPPC/CHEMS (1:1) and DPPC/SSD (1:1) mixtures were compared with that of DPPC (Fig. 4).

Although the magnitude of the red shift is relatively small compared to the peak width (Asada et al., 2004), addition of CHOL, CHEMS and SSD in DPPC substantially induced the red shift of V_s P=O (from 1247.78 to 1241.99, 1240.07, 1235.21 cm^{-1}, respectively) and V_{as} P=O (from 1469.56 to 1465.71, 1467.64, 1465.71 cm^{-1}, respectively). We know that the asymmetry flexual vibration of the quaternary ammonium of DPPC is a small or side peak at 1670–1640 cm^{-1} (Peng, 1998). We can read from Fig. 4 that CHOL and SSD did not conceal the peak as there is no static electronic interaction between the hydroxyl groups and the quaternary ammonium of DPPC. While in the FT-IR spectrogram of the DPPC/CHEMS (1:1) mixture, the small peak (at 1670–1640 cm^{-1}) was absent, suggesting electrostatic interaction between the carboxyl group of CHEMS and the quaternary ammonium of DPPC.

3.4. SSD complex with CHOL but not with CHEMS

If SSD interacts with CHOL or CHEMS, it will insert lipid bilayers and ultimately disrupt the membrane structure of DPPC/CHOL (10:4)- or DPPC/CHEMS (10:4)-liposomes, causing large lipid aggregates to form and increasing the sedimentation and clarity of the supernatant of the liposome suspension.

To exclude an increase in clarity caused by liposome aggregation and sedimentation, distilled water was added. The results (Fig. 5) indicated there was no change in turbidity, which meant DPPC/CHOL (10:4)- and DPPC/CHEMS (10:4)-liposomes did not undergo sedimentation during the period of the experiment. After addition of SSD to DPPC/CHOL (10:4)- or DPPC/CHEMS (10:4)-liposomes, there was significant sedimentation for DPPC/CHOL (10:4)-liposomes and no turbidity change was observed for DPPC/CHEMS (10:4)-liposomes, which meant that SSD did not interact with CHEMS (Fig. 5).

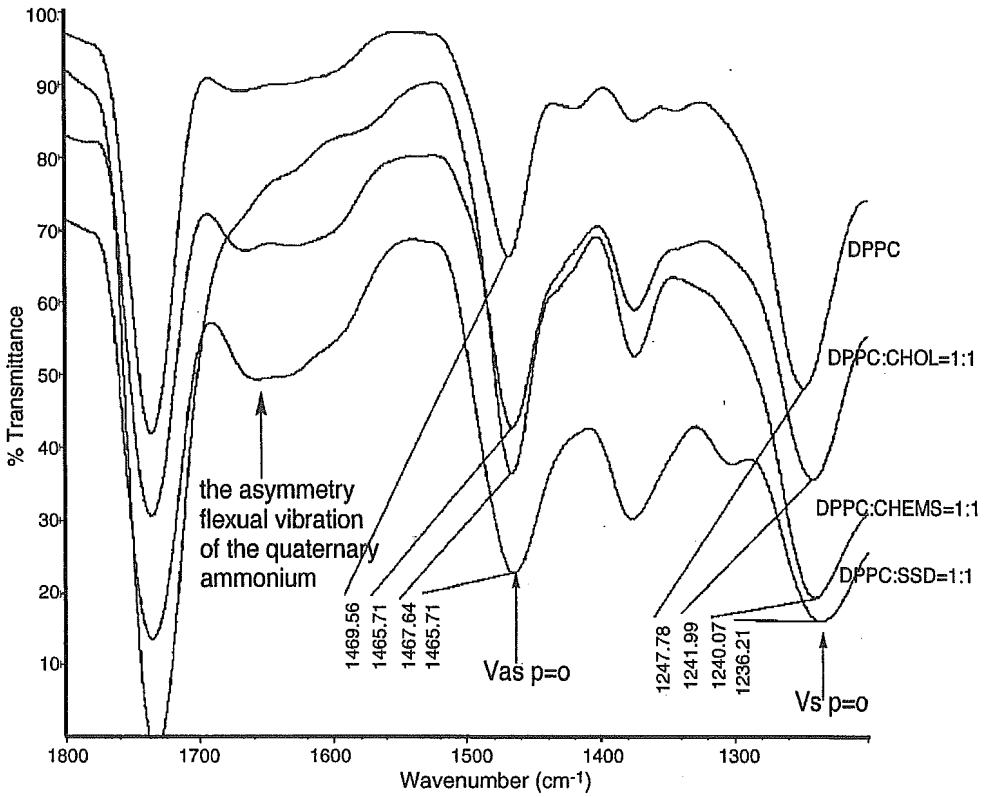

Fig. 4. FT-IR combinational spectrograms of DPPC mixtures with CHOL, CHEMS and SSD (1:1, molar ratio) between 1800 and 1200 cm^{-1}.

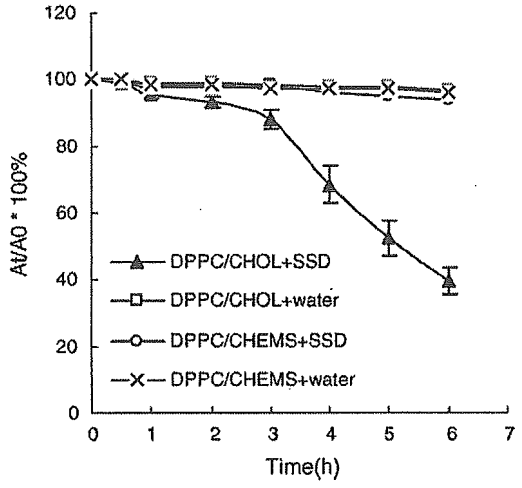

Fig. 5. Relative turbidity curve of DPPC/CHEMS (10:4)- and DPPC/CHOL (10:4)-liposomes (with a DPPC concentration of 0.5 mg/ml) after adding 200 μg/ml SSD suspension or distilled water. (The data are presented as mean ± S.D., $n = 3$.)

3.5. Hemolytic curve of SSD-liposomes

It seemed that DPPC/CHEMS/SSD (10:4:1)-liposomes could reduce the hemolytic activity of SSD in contrast to the SSD solution or the liposomes without CHEMS (DPPC/SSD (10:1)-liposomes) (Fig. 6). The liposomes that incorporated DSPE-PEG (DPPC/CHEMS/DSPE-PEG/SSD (10:4:0.5:1)-liposomes) showed the greatest ability to reduce the hemolytic activity. Thus, the SSD-liposomes should contain DSPE-PEG.

4. Discussion

In the present study, a value of the maximal transition temperature of 39.52 °C was observed for DPPC (Fig. 2), while a more usual literature value of 41 °C was reported. The great difference may be attributed to different lipid concentration used, different running conditions and different machines. We have found that

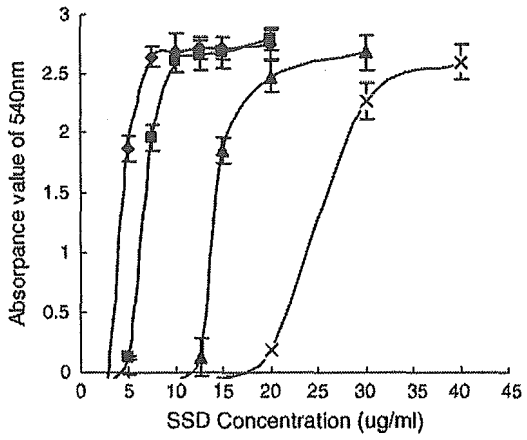

Fig. 6. Hemolytic curve of SSD solution and SSD-liposomes (with a lipid concentration of 2.5 mg/ml) on rabbit erythrocyte in vitro. (The data are presented as mean ± S.D., $n = 3$.) (◆): SSD solution, (■): DPPC/SSD (10:1)-liposomes, (▲): DPPC/CHEMS/SSD (10:4:1)-liposomes, (×): DPPC/CHEMS/DSPE-PEG/SSD (10:4:0.5:1)-liposomes.

a less concentrated liposome suspension of 20 mg/ml of DPPC (10 μl equal to 0.2 mg of DPPC) produced a phase transition temperature of 40.5 °C, which is similar to the literature value. But, lower concentration of DPPC resulted in lower enthalpy value and lower sensitivity, therefore, 100 mg/ml of DPPC were employed during the experiments and the results allowed meaningful comparison since the experimental conditions were strictly controlled as the same for each other.

Addition of CHOL, CHEMS and SSD to DPPC-liposomes decreased the T_m and ΔH values of DPPC (Fig. 2 and Table 1), which accorded with the finding that introduction of a hydrophobic molecular within the lipid bilayers produces a decrease in T_m and ΔH (Mabrey and Sturtevant, 1976). As mentioned in the literature (Yang and Su, 1998; Wang, 1997), when above the phase transition temperature, the membrane fluidity drops when the area of the endothermic peak (ΔH value) decreases and the T_m value increases. Since the ΔH is markedly decreased as compared with the T_m, the reduction of ΔH is much more dominant while the decrease in T_m is negligible in membrane stabilization.

CHEMS could reduce the fluidity of the liposomal membrane according to the ΔH reduction (1.16 J/g for DPPC/CHEMS (10:1)-liposomes compared to 5.26 J/g for DPPC/CHOL (10:1)-liposomes), suggesting that CHEMS possesses more stabilization ability than CHOL. The result was supported by the calcein release study.

The hydroxyl group of CHOL and the sugar moiety of SSD can both form a hydrogen bond with the P=O bond of DPPC (Peng, 1998; Shimizu et al., 1996), which caused the red shift of V_s P=O and V_{as} P=O (Fig. 4). As for CHEMS, the red shift of V_s P=O and V_{as} P=O may be due to the fact that the carbonyl group of CHEMS can form a hydrogen bond with the P–OH bond of DPPC, and therefore affect the vibration of the P=O bond.

CHOL and CHEMS had a similar effect on the red shift of V_s P=O, while SSD had the strongest effect on the red shift of V_s P=O due to abundant hydroxyl groups on the sugar moiety of SSD. But maybe because of the small molecular volume of the hydroxyl group and succinic acid, together with the deep-anchored sterol ring reducing the hydrocarbon movement (Massey, 1998), they may fill the polar headspace of lipid bilayers and thus increase the membrane stability. As for SSD, although it had the strongest hydrogen interaction with the polar head of DPPC, it may disrupt the lipid arrangement due to the large molecular volume of the sugar moiety (Muramatsu et al., 1999), thus increasing the membrane fluidity.

Fig. 7 illustrates the proposed mechanism of interaction mechanism of DPPC with CHOL, CHEMS and SSD. The hydroxyl group of CHOL and the sugar moiety of SSD could form a hydrogen bond with the phosphorus oxygen double bond (P=O) of DPPC, then the electron cloud around the oxygen of P=O will migrate to the hydroxyl group, decreasing the polarity of P=O bond, and causing the red shift of the stretching vibration of P=O.

As for CHEMS, the carbonyl group of CHEMS might have hydrogen bond interaction with the P–OH bond of DPPC, then the electron cloud around the hydroxyl group of P–OH might become much more intense, and the increased electron cloud around the hydroxyl group of P–OH will migrate to the phosphorus atom of P–OH. Therefore, the decrease in the polarity of the P=O bond may cause a red shift. In addition, electrostatic interaction may exist between the carboxyl group of CHEMS and the quaternary ammonium of DPPC.

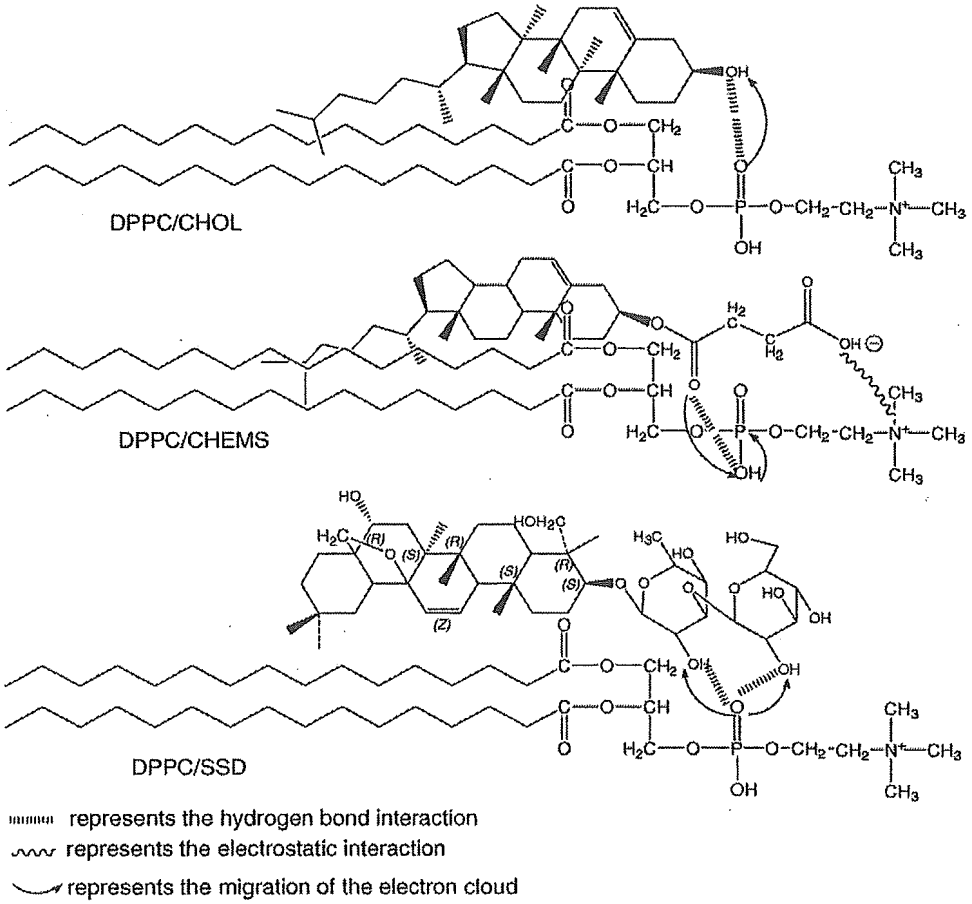

Fig. 7. Schematic diagram of interaction of DPPC with CHOL, CHEMS and SSD.

CHEMS can possess both hydrogen bond interaction and electrostatic interaction with DPPC membrane while CHOL only has hydrogen bond interaction. This difference may make the membrane of DPPC/CHEMS-liposomes more compact and steady than that of DPPC/CHOL-liposomes, being supported by the reduction of ΔH in DSC and low calcein release. In contrast, Massey (1998) reported that CHEMS could extend across one monolayer of the bilayer and partially interdigitate into the opposing monolayer of the bilayer, resulting in less membrane stabilization than CHOL by fluorescence polarization. From our study we hypothesized that the whole succinic group of CHEMS might fit into the polar head of DPPC and the sterol ring might be in the same position as that of CHOL.

CHEMS turned out to be a unique membrane stabilizer in SSD-liposomes due not to interaction with SSD as illustrated in Fig. 5. The reason may be ascribed to the succination of the hydroxyl group of CHOL, blocking recognition by SSD.

Further, CHEMS will find great use in the preparation of liposomes containing cholesterol-dependent hemolytic saponins. The incorporation of SSD into liposomes contained CHEMS could reduce its hemolytic activity (Fig. 6), because: SSD was incorporated in the lipid bilayers of liposomes, and liposomes containing CHEMS were negatively charged due to the presence of carboxylic acid residue and would experience repulsive interactions with erythrocyte membranes. In addition, reduced hemolytic activity of SSD-liposomes was observed on adding DSPE-PEG,

which may further exert a steric hindrance between liposome membranes and erythrocyte membranes.

This study has shown that CHEMS was more effective than CHOL in increasing DPPC membrane stability since CHEMS may possess both hydrogen bond interaction and electrostatic interaction with DPPC membrane while CHOL only has hydrogen bond interaction. Furthermore, CHEMS can be used as a unique membrane stabilizer in liposomes containing SSD. SSD-liposomes contained CHEMS and DSPE-PEG could greatly decrease the hemolytic activity of SSD.

Acknowledgment

This research was supported by a grant (30271520) from the National Science Foundation of China.

References

Abe, H., Orita, M., Konishi, H., Arichi, S., Odashima, S., 1986. Effects of saikosaponin-d on aminonucleoside nephrosis in rats. Eur. J. Pharmacol. 120, 171–178.

Asada, M., Takahashi, H., Okamoto, H., Tanino, H., Danjo, K., 2004. Theophylline particle design using chitosan by the spray drying. Int. J. Pharm. 270, 167–174.

Cheng, H.F., 1994. Saikasaponins for the treatment of nephritis. World Pharm. Newslett. 12, 24–25.

Cheng, S., Peng, C.E., Yang, M.J., 1999. The experimental research of Saikasaponins on the proliferation and matrix synthesis of hepatocyte. Chin. J. Basic Med. Tradit. Chin. Med. 28, 21–25.

Dumas, D., Muller, S., Gouin, S.F., Baros, F., Viriot, M.L., Stoltz, J.F., 1997. Membrane fluidity and oxygen diffusion in cholesterol-enriched erythrocyte membrane. Arch. Biochem. Biophys. 341, 34–39.

Fariss, M.W., Bryson, K.F., Hylton, E.E., Lippman, H.R., Stubin, C.H., Zhao, X.G., 1993. Protection against carbon tetrachloride-induced hepatotoxicity by pretreating rats with the hemisuccinate esters of tocopherol and cholesterol. Environ. Health Perspect. 101, 528–536.

Gregoriads, G., 1988. Liposomes as Drug Carriers: Recent Trends and Progress. Wiley, New York.

Ismail, M., Hafez, P., Cullis, R., 2000. Cholesteryl hemisuccinate exhibits pH sensitive polymorphic phase behavior. Biochim. Biophy. Acta 1463, 107–114.

Kida, H., Akao, T., Meselhy, M.R., Hattori, M., 1998. Metabolism and pharmacokinetics of orally administered saikosaponin b1 in conventional, germ-free and *Eubacterium* sp. A-44-infected gnotobiote rats. Biol. Pharm. Bull. 21, 588–593.

Kuhn, R.W., Schrader, W.T., Smith, R.G., O'Malley, B.W., 1975. Progesterone binding components of chick oviduct. J. Biol. Chem. 250, 4220–4228.

Lai, M.Z., Duzgunes, N., Szoka, F.C., 1985. Effects of the replacement of the hydroxyl group of cholesterol and tocopherol on the thermotropic behavior of phospholipid membranes. Biochemistry 24, 1646–1653.

Mabrey, S., Sturtevant, J.M., 1976. Investigation of phase transitions of lipids and lipid mixtures by high sensivity differential scanning calorimetry. Proc. Natl. Acad. Sci. U.S.A. 73, 3862–3866.

Massey, J.B., 1998. Effect of cholesteryl hemisuccinate on the interfacial properties of phosphatidylcholine bilayers. Biochim. Biophy. Acta 1415, 193–204.

Muramatsu, K., Takayama, K., Maitani, Y., 1999. The relationship between the rigidity of the liposomal membrane and the absorption of insulin after nasal administration of liposomes modified with an enhancer insulin in rabbit. Drug Dev. Ind. Pharm. 25, 1099–1105.

Nakamura, T., Kuriyama, M., Kosuge, E., 1993. Effect of saikosaponin on the production of platelet activating factor in human neutrophils. Ann. N.Y. Acad. Sci. 685, 572–579.

Peng, S.Q., 1998. Spectrogram Analysis of Drugs. Beijing Medical University Publishing House, Beijing, China, pp. 106–113.

Ray, S.D., Mumaw, V.R., Raje, R.R., Fariss, M.W., 1996. Protection of acetaminophen induced hepatocellular apoptosis and necrosis by cholesteryl hemisuccinate pretreatment. J. Pharmacol. Exp. Ther. 279, 1470–1483.

Se'rgio, S., Moreira, J.N., Cristina, F., 2004. On the formulation of pH-sensitive liposomes with long circulation times. Adv. Drug Delivery Rev. 56, 947–965.

Shimizu, K., Maitani, Y., Takayama, K., Nagai, T., 1996. Characterization of dipalmitoylphosphatidylcholine liposomes containing a soybean derived sterylglucoside mixture by differential scanning calorimetry, fourier transform infrared spectroscopy and enzymatic assay. J. Pharm. Sci. 85, 741–744.

Skornick, Y.G., Rong, G.H., Sindelar, W.F., Richert, L., Klausner, J.M., Rozin, R.R., Shinitzky, M., 1986. Active immunotherapy of human solid tumor with autologous cells treated with cholesteryl hemisuccinate. A phase I study. Cancer 58, 650–654.

Szoka, F., Papahadjopoulos, D., 1978. Procedure for preparation of liposomes with large internal aqueous space and high capture by reverse-phase evaporation. Proc. Natl. Acad. Sci. U.S.A. 75, 4194–4198.

Ushio, Y., Abe, H., 1991. Effect of saikosaponin-d on the function and morphology of macrophages. Int. J. Immunopharmacol. 13, 493–499.

Wang, B., 1997. The effect of cholesterol on the biomembrane fluidity. Acta Acad. Med. Guangxi 14, 34–36.

Wang, X.K., 1992. Tian Rang Yao Wu Hua Xue. People's Medical Publishing House, Beijing, China, pp. 524–541.

Wen, X.G., 1993. The transformation of Saikasaponin in xiong dan fu gan ning. Zhong ChengYao 3, 16–18.

Yang, L., Su, W.A., 1998. DSC, ESR and FP for the fluidity of membrane lipids. Acta Univ. Agric. Boreali-occidentalis 26, 99–104.

Yokoyama, H., Hiai, S., Oura, H., 1984. Effect of saikosaponins on dexamethasone suppression of the pituitary–adrenocortical system. Chem. Pharm. Bull. 32, 1224–1227.

Zhang, G.J., Liu, H.W., Yang, L., Zhong, Y.G., Zheng, Y.Z., 2000. Influence of membrane physical state on the lysosomal proton permeability. J. Membr. Biol. 175, 53–62.

Zhang, T.G., 1993. The study of Japanese Bupleurum formulation on the treatment of nephritis. Chin. J. Chin. Mater. Med. 18, 753–756.

Zhong, G.Y., Xue, K.X., Yuan, Y.W., Yan, J.S., 1993. Zhong Yao Zhi, 2nd ed. People's Medical Publishing House, Beijing, China, pp. 486.

Zhou, Q.L., Zhang, Z.Q., Nagasawa, T., Hiai, S., 1996. The structure activity relationship of saikosaponins and glycyrrhizin derivatives for Na^+, K^+-ATPase inhibiting action. Acta Pharm. Sin. 31, 496–501.

Available online at www.sciencedirect.com
SCIENCE DIRECT
Journal of Controlled Release 104 (2005) 313–321
journal of controlled release
www.elsevier.com/locate/jconrel

Influence of serum and albumins from different species on stability of camptothecin-loaded micelles

Praneet Opanasopit[a], Masayuki Yokoyama[b,*], Masato Watanabe[c], Kumi Kawano[c], Yoshie Maitani[c], Teruo Okano[a]

[a]*Institute of Advanced Biomedical Engineering and Science, Tokyo Women's Medical University, Kawada-cho 8-1, Shinjuku-ku, Tokyo 162-8666, Japan*
[b]*Kanagawa Academy of Science and Technology, KSP Bldg. East 404, Sakado 3-2-1, Takatsu-ku, Kawasaki-shi, Kanagawa-ken, 213-0012, Japan*
[c]*Institute of Medical Chemistry, Hoshi University, Ebara 2-4-41, Shinagawa-ku, Tokyo 142-8501, Japan*

Received 10 August 2004; accepted 18 February 2005
Available online 9 April 2005

Abstract

Stability of CPT free drug and CPT-loaded polymeric micelles forming from poly (ethylene glycol)-poly (benzyl aspartate-69) block copolymer in the presence of serum and purified serum albumins were investigated by reverse-phase HPLC and GPC. The hydrolysis of CPT and CPT-loaded micelles follows pseudo-first-order kinetics. The observed hydrolysis rate constants for CPT and CPT-loaded micelles were 7.4×10^{-3} min^{-1} and 0.7×10^{-3} h^{-1}, corresponding to an increase in half-life of CPT from 94 min to 990 h, respectively. The half-lives of CPT lactone hydrolysis of CPT-loaded micelles in the presence of BSA were significantly longer than the control whereas in the presence of HSA and serum was shorter than the control, and the similar results were obtained from GPC analyzed for micelles stability. This result suggested that the stability of CPT-loaded micelles was significantly decreased only in the presence of human albumin and serum. These were corresponded to the results of CPT free drug observed in the presence of albumins or serum. BSA significantly retarded the CPT lactone ring opening as compared with the control. On the other hand, HSA and serum showed rapid CPT lactone ring opening. This was probably due to preferential HSA binding to the carboxylate form resulting in a change in the lactone–carboxylate equilibrium, whereas, BSA did not bind to the lactone form, but might promote the self-aggregation of CPT and binding to the hydrophobic inner core of the micelles, resulting in enhanced stability of CPT-loaded micelles. MSA did not affect the stability of micelles.
© 2005 Elsevier B.V. All rights reserved.

Keywords: Serum; Albumin; Polymeric micelles; Camptothecin; Stability

* Corresponding author. Tel.: +81 44 819 2093; fax: +81 44 819 2095.
E-mail addresses: masajun@ksp.or.jp (M. Yokoyama), tokano@abmes.twmu.ac.jp (T. Okano).

0168-3659/$ - see front matter © 2005 Elsevier B.V. All rights reserved.
doi:10.1016/j.jconrel.2005.02.014

1. Introduction

A major problem currently associated with systemic drug administration is its even biodistribution throughout the body, resulting in the lack of specificity in its pharmacological activity to target cells. In addition, to reach the site of action drug has to overcome several biological barriers by which it may be inactivated. Camptothecin (CPT) is a potent, anticancer agent acting through the inhibition of topoisomerase I during the S-phase of the cell cycle [1]. It exists in two forms depending on the pH value, namely, an active lactone form at pH below 5 and an inactive carboxylate form at basic pH (Fig. 1a) [2]. At physiological pH, most CPT molecules exist in the inactive carboxylate form. The stable lactone form of CPT is critical for its anticancer activity. In addition, the ring opening carboxylate form shows poorer diffusibility through the lipid bilayer than the lactone form. Therefore, factors influencing a lactone–carboxylate equilibrium within the CPT molecule are clearly important determinants of the agent's function. Human serum albumin (HSA) was shown to bind preferentially with the carboxylate form, resulting in the lactone ring opening more rapidly [3,4]. However, serum albumins from other species were found to bind CPT carboxylate not as tightly as HSA [5]. In addition, Nabiev et al. [6,7] reported that BSA did not participate in binding of the lactone, carboxylate, or self-aggregate of CPT. This fact may result in differences between clinical trials and animal experiments of this drug. Red blood cells stabilize the biologically active form of CPT by allowing the lactone ring to partition into lipid bilayers, thereby protecting the moiety from hydrolysis [3]. Nabiev et al. [6,7] discovered a novel effect certainly influencing the biological activity of CPT: at low concentrations in aqueous buffer solutions, stable J-type aggregates formed by the stacking interaction between the quinoline rings of the CPT chromophores with the inverse position of the nitrogen atoms. This self-aggregation partially prevents hydrolysis of the lactone ring at neutral pH values and J-aggregates were found to penetrate within the cells with much higher efficiency than the monomers of the drug.

A number of delivery systems are under development for targeted and controlled delivery of drugs. When entering into the systemic circulation by intravascular administration or through absorption at the administration site, a delivery system carrying pharmaceuticals encounters blood cells and plasma proteins before reaching its target cells. Serum proteins, erythrocytes and other blood cells can bind to the drug carriers leading to an alteration in its physicochemical properties such as particle size and electrical charge [8]. If it interacts with those blood components,

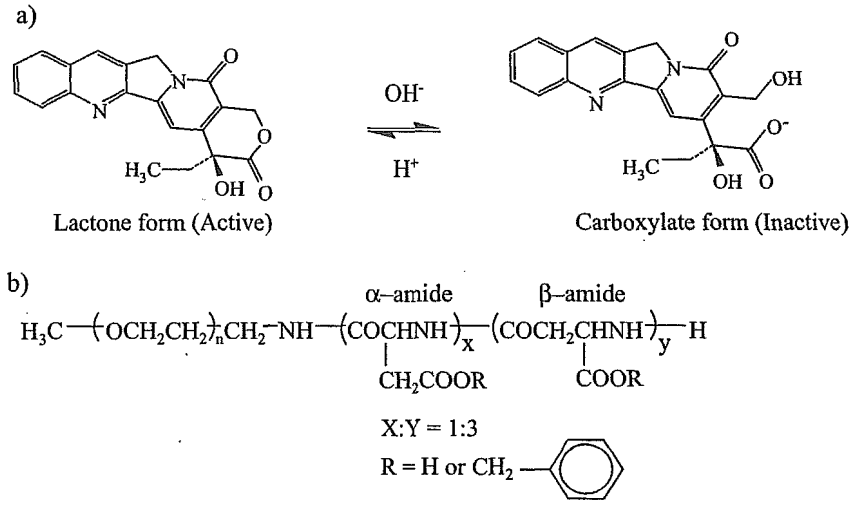

Fig. 1. (a) Chemical structure of camptothecin (CPT) two forms depending on the pH value, namely, an active lactone form at pH below 5 and an inactive carboxylate form at basic pH. (b) Chemical structure of poly(ethylenglycol)-poly(benzyl aspartate 69) block copolymers.